8-2018

An Enthalpy Model for the Dynamics of a Deltaic System Under Base-Level Change

William Anderson
Montclair State University

Abstract

Fluvial deltas are composites of two primary sedimentary environments: a depositional fluvial region and an offshore region. The fluvial region is defined by two geomorphic moving boundaries: an alluvial-bedrock transition (ABT), which separates the sediment prism from the non-erodible bedrock basement, and the shoreline (SH), where the delta meets the ocean. The trajectories of these boundaries in time and space define the evolution of the shape of the sedimentary prism, and are often used as stratigraphic indicators, particularly in seismic studies, of changes in relative sea level and the identification of stratigraphic sequences. In order to better understand the relative role of sea-level variations, sediment supply, and basin geometry on the evolution of the ABT and SH, we develop a forward stratigraphic model that captures the dynamic behavior of the fluvial surface and treats the SH and ABT as moving boundaries (i.e., internal boundaries whose location must be determined as part of the solution to the overall morphological evolution problem). This forward model extends a numerical technique from heat transfer (i.e., enthalpy method), previously applied to the evolution of sedimentary basins, to account for sea-level variations, including eustatic sea-level cycles. In general, model results demonstrate the importance of the dynamics of the fluvial surface on the system response under a wide range of parameter values. In particular, model results suggest that time lags in the ABT response during sea-level cycles can result in river incision during the sea-level rise. These results can have important implications for the reconstruction of past sea-level changes from the stratigraphic record of sedimentary basins.

MONTCLAIR STATE UNIVERSITY

An Enthalpy Model for the Dynamics of a Deltaic System Under Base-Level Change

by

William Anderson

A Master's Thesis Submitted to the Faculty of

Montclair State University

In Partial Fulfillment of the Requirements

For the Degree of

Master of Science

August 2018

College of Science and Mathematics

Department of Mathematical Sciences

Thesis Committee:

[redacted]

Dr. Jorge Lorenzo-Trueba
Thesis Sponsor

[redacted]

Dr. Eric Forgoston
Committee Member

[redacted]

Dr. Arup Mukherjee
Committee Member

AN ENTHALPY MODEL FOR THE DYNAMICS OF A DELTAIC SYSTEM UNDER BASE-LEVEL CHANGE

A THESIS

Submitted in partial fulfillment of the requirements
for the degree of Master of Science

by

William Anderson
Montclair State University
Montclair, NJ
2018

Contents

List of Figures

1 Introduction

Coastal areas such as deltas and continental margins include composites of several primary environments, including a depositional fluvial region and an offshore region, that generally resemble a triangular prism in longitudinal section, superimposed upon a relatively flat basement profile (Figure 1a; Paola, 2000; Posamentier et al., 1992). This triangular sedimentary prism presents three geomorphic boundaries or vertices: the alluvial-bedrock transition (ABT), which separates the bedrock (or basement) from the depositional fluvial region, the shoreline (SH), which separates the fluvial region from the subaqueous depositional region, and the submarine toe where the submarine sediment wedge re-intersects with the basement. Changes in the length of the depositional fluvial domain occur via transgression/regression at the SH and/or coastal onlap/offlap at the ABT (Figure 1). These changes are in general a function of the sediment supply to the sedimentary prism, the efficacy of the sediment transport and deposition along the fluvial surface, and relative sea-level variations (i.e., the combination of eustatic sea level changes and subsidence). For instance, a high sediment supply relative to the length of the fluvial surface and the accommodation created by relative sea-level rise results in an increase in elevation (i.e., river aggradation) of the depositional surface, and an overall lengthening of the sedimentary prism (Figure 1b). A combination of relative sea-level fall with low sediment supply, however, typically results in a decrease in elevation (i.e., river degradation) of the fluvial surface (Figure 1c). Additionally, Muto and Steel (2002) found that a low sediment supply relative to the length of the fluvial surface and the rate of relative sea-level rise can lead to a break in the triangular geometry of the sedimentary prism (Figure 1d).

Patterns of SH transgression/regression and coastal onlap/offlap in the stratigraphic record (Figure 1) can potentially allow for reconstruction of a basin's history of sediment supply and paleo–sea level. To tackle this inverse problem, the migration of the internal boundaries that describe the evolution of the system (e.g., ABT, SH) have to be determined as a part of the solution to the overall morphological evolution problem (Lorenzo-Trueba et al., 2013, 2009; Lorenzo-Trueba and Voller, 2010; Marr et al., 2000; Swenson et al., 2000). Similar to the one phase Stefan melting problem in which one of the domain boundaries is the moving solid/liquid front (Crank, 1984), Swenson et al. (2000) applied this framework to the formation and evolution of sedimentary basins. In particular, these authors used an analogy between heat and sediment diffusive transport to describe the movement of the SH under varying conditions of sediment supply and relative sea level. Follow-up work by Voller et al. (2004) found that in the particular case of constant sediment supply and a fixed sea level, the problem presented by Swenson et al. (2000) allows for a closed-form analytical solution. Based on Voller et al. (2004), Capart et al. (2007), and Lai and Capart (2007) developed analytical solutions in which the ABT and the SH were treated as independent moving boundaries. Lorenzo-Trueba et al. (2009) expanded on this work by developing an analytical solution able to track both the ABT and the SH under conditions of constant sediment supply and fixed sea-level. Lorenzo-Trueba et al. (2009) also validated this solution against flume experiments under a range of system parameters.

Although simplified solutions can increase the clarity and insights the model facilitates, moving boundary problems only have analytical solutions in a limited range of scenarios. In order to study more general cases, different numerical methods have been developed for the dual ABT and SH moving boundary problem (Lorenzo-Trueba and Voller, 2010; Parker et al., 2008; Voller et al., 2006). Parker et al. (2008) developed a deforming grid method, based on a Landau front-fixing approach, able to track both the ABT and the SH under constant sea-level rise in a one-dimensional setting. A drawback of the deforming grid method for the sediment delta problem, however, is that there is not an obvious path toward the solution of two-dimensional problems. Voller et al. (2006) developed an enthalpy-like solution able to operate on a fixed grid under constant sea level, in which the moving boundary of interest is the SH. Lorenzo-Trueba and Voller (2010) extended the enthalpy-like solution to account for the migration of both the ABT and SH. Despite these recent developments, however, to date all numerical solutions have been restricted to either a fixed sea level or constant sea-level rise scenarios. The only attempt to solve the problem under sea-level cycles was by Lorenzo-Trueba et al. (2013), who developed an integral approximation of the Exner equation assuming a quadratic fluvial surface profile. This solution, however, is not able to account for full cycles of transgression and regression (only cases where transgression follows regression). Thus, the first objective of this paper is to extend the enthalpy solution from Lorenzo and Voller (2010) to account for sea-level cycles, as well as cycles of SH transgression/regression. Second, we investigate potential modes of coastal behavior under sea-level cycles and a wide range of system parameters.

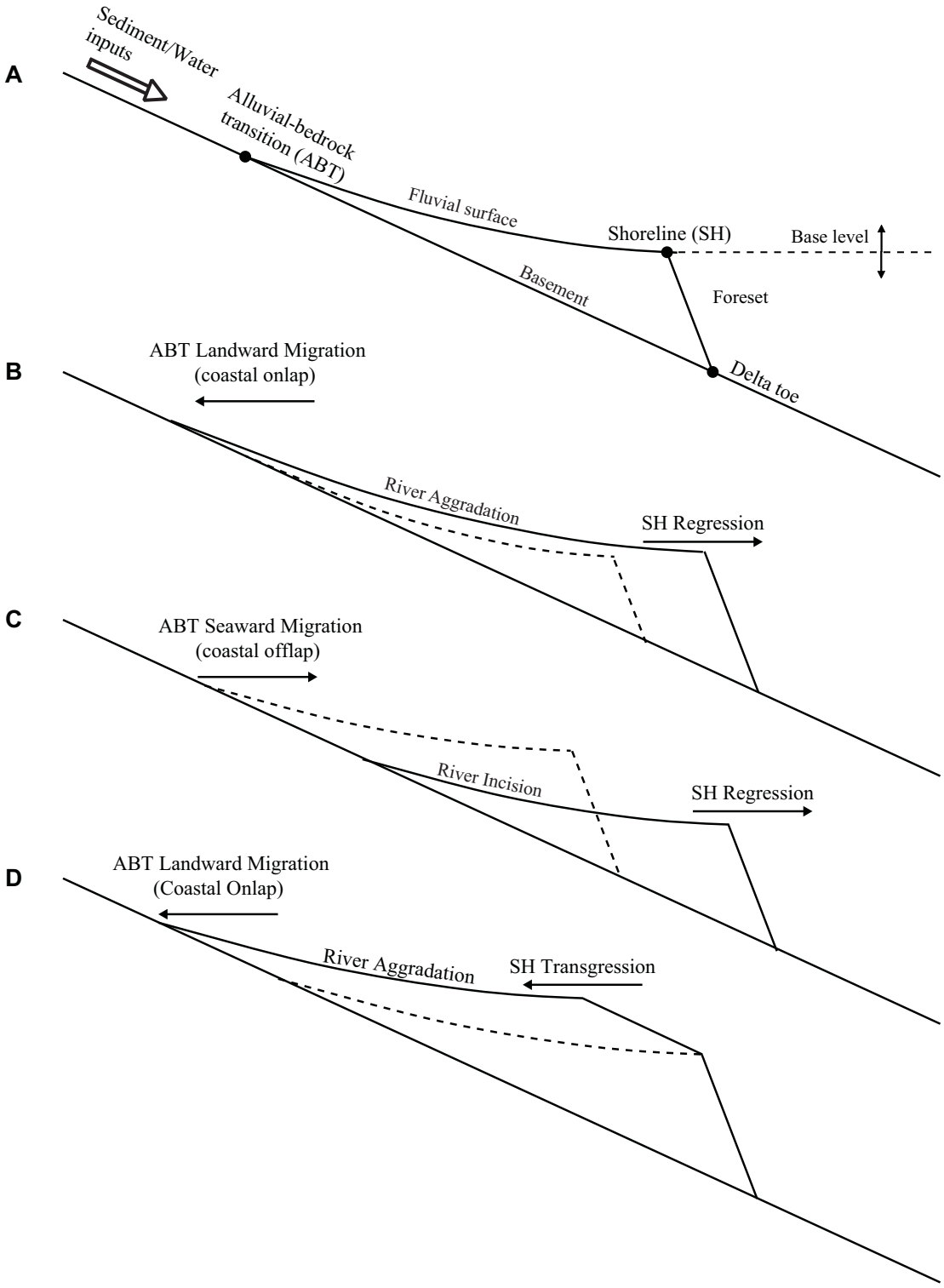

Figure 1: Idealized alluvial deltaic system longitudinal profile. The terminology used to describe the system is shown in (a). Possible scenarios of boundary movement are shown in (b), (c), and (d). In (d) we see the scenario described as autobreak where there is a shift in delta's geometry.

2 The Dual Moving Boundary Problem

2.1 Equations

Similarly to many previous physically validated modeling studies (Fagherazzi and Overeem, 2007; Lorenzo-Trueba et al., 2013; Lorenzo-Trueba and Voller, 2010; Marr et al., 2000; Paola et al., 1992; Parker and Muto, 2003; Postma et al., 2008; Swenson et al., 2000; Swenson and Muto, 2007), we assume that sediment flux is a function of the local fluvial slope. The simplest form of this model is to assume that the flux, q, is directly proportional to the fluvial slope, i.e.,

$$q = -\nu \frac{\partial h}{\partial x} \tag{1}$$

where x positive in the seaward direction, $x = 0$ is located at the intersection between the initial sea-level and the basement, h is the elevation of the fluvial surface respect to sea-level (Figure 2), and ν is the 'fluvial diffusivity', which scales with the water discharge and has units of length squared over time (Paola, 2000). With the above assumption for the sediment transport, a governing equation is derived by using the unit flux definition (1) in the Exner equation (Paola and Voller, 2005) for the mass balance in the sediment wedge, to arrive at the diffusion equation

$$\frac{\partial h}{\partial t} = \nu \frac{\partial^2 h}{\partial x^2}, \qquad r(t) \leq x \leq s(t). \tag{2}$$

The boundary conditions for this dual moving boundary problem are:

$$h\Big|_{x=r} = -r\beta \tag{3a}$$

$$h\Big|_{x=s} = Z \tag{3b}$$

$$\nu \frac{\partial h}{\partial x}\Big|_{x=r} = -q_0 \tag{3c}$$

$$\nu \frac{\partial h}{\partial x}\Big|_{x=s} = \begin{cases} D(x,t)\dfrac{dw}{dt}, & \dfrac{dw}{dt} > 0 \\ 0, & \dfrac{dw}{dt} \leq 0 \end{cases} . \tag{3d}$$

The first two conditions are obtained by matching the fluvial surface with the bedrock at the ABT (3a) and with the sea level at the SH (3b). The extra boundary conditions (3c) and (3d) are required to track the horizontal positions of the boundaries, the SH $x = s(t)$ and the ABT $x = r(t)$. Equation (3c) imposes a given sediment input at $x = r(t)$ and equation (3d), analogous to the Stefan condition in heat transfer, expresses the balance of sediment at the shoreline originally proposed by Swenson et al (2000), where the rate of migration of the foreset toe is defined as $dw/dt = ds/dt + 1/\psi \cdot dZ/dt$ and $D(t)$ is the basin depth. In the particular case in which the shoreface toe only migrates seawards (i.e. $dw/dt > 0$), the system maintains the wedge geometry depicted in Figure 1, and we can define the basin depth as $D(t) = \psi/(\psi - \beta) \cdot (s\beta + Z)$. In contrast, when the shoreface

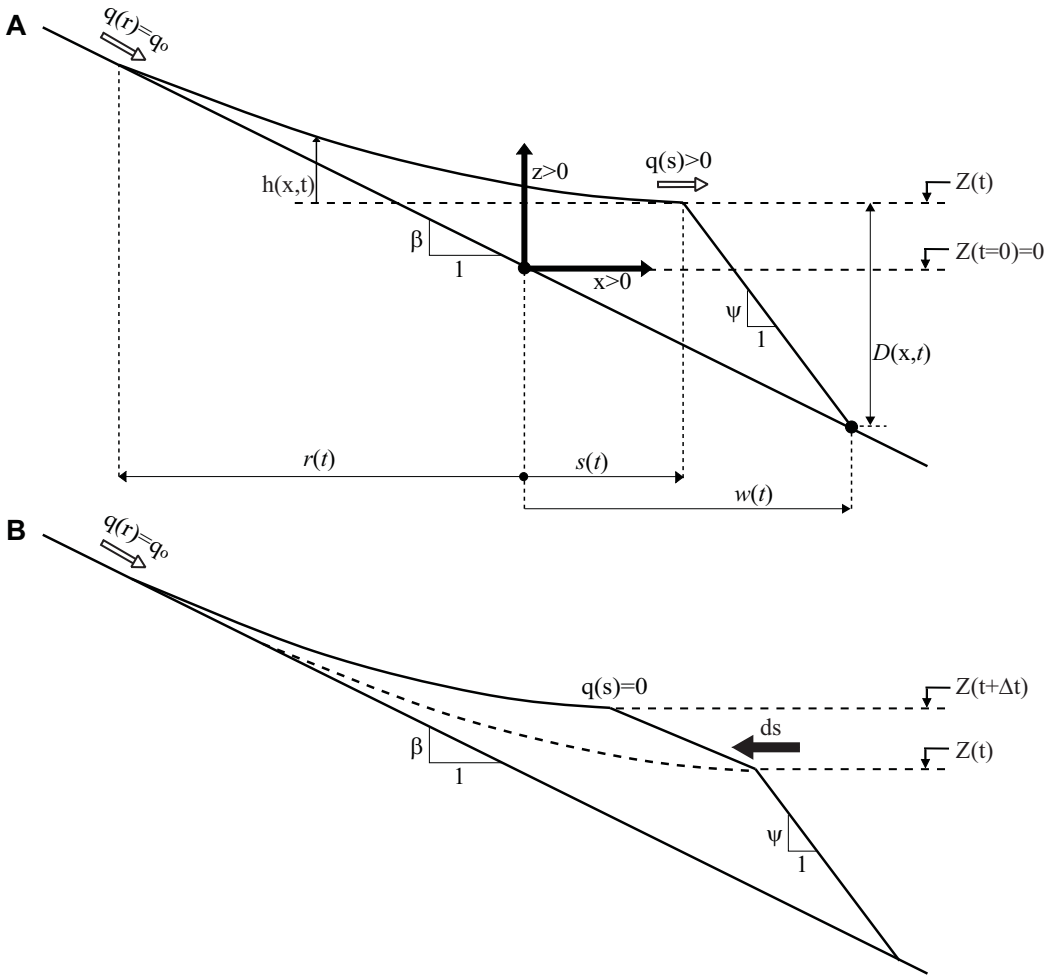

Figure 2: (a) Delta longitudinal profile with the state variables. (b) Sketch for autobreak.

toe migrates landwards (i.e.,$dw/dt \leq 0$), all the sediments are accumulated in the subaerial portion of the wedge and the SH flux is identically zero. Under this condition, the SH detaches from the subaqueous foreset (Figure 2b), a condition previously defined as 'autobreak' (Muto and Steel 2002).

In general, with a given initial geometry: $s(0) =, r(0) = h(0, x) = 0$, equations (1-3) are sufficient to describe the fluvial elevation and the movements of the ABT and SH during sea-level fall or sea-level rise.

2.2 A Dimensionless Form

In order to reduce the number of controlling parameters to a minimum, we rewrite the governing equations (1-3) in dimensionless form. Toward this end the following scaling is introduced

$$x^d = \frac{x}{l}, t^d = \frac{t}{\tau}, s^d = \frac{s}{l}, r^d = \frac{r}{l}, Z^d = \frac{Z}{l\beta}, h^d = \frac{h}{l\beta}, D^d = \frac{D}{l\beta}, q^d = \frac{q\tau}{l^2\beta} \qquad (4)$$

where l is the horizontal scale (e.g., a characteristic basin length), $l\beta$ is the vertical scale, and $\tau = l^2/\nu$ is the 'basin equilibrium timescale' defined by Paola et al. (1992). The scaling in (4) leads to two dimensionless groups: the ratio of the fluvial to the bedrock slope at the ABT

$$R_{ab} = -\left.\frac{\partial h}{\partial x}\right|_{x=r} = \frac{q_0}{\beta\nu} \tag{5}$$

and the slope ratio at the SH

$$R_{sh} = \frac{\psi}{\psi - \beta}. \tag{6}$$

In equation (6), given that the foreset slope ψ is typically orders of magnitude larger than the basement slope β, we assume $R_{sh} \sim 1$ (Edmonds et al., 2011; Lorenzo-Trueba et al., 2013, 2009; Lorenzo-Trueba and Voller, 2010; Swenson and Muto, 2007). Consequently, we assume that autobreak (i.e., the abandonment of the subaqueous foreset) and the shift from regression to transgression occur simultaneously. In this way, dropping the d superscript for convenience of notation, the dimensionless volume balance governing equation becomes:

$$\frac{\partial h}{\partial t} = \frac{\partial^2 h}{\partial x^2}, \qquad r(t) \leq x \leq s(t) \tag{7}$$

with conditions

$$\left. h \right|_{x=r} = -r \tag{8a}$$

$$\left. h \right|_{x=s} = Z \tag{8b}$$

$$\left.\frac{\partial h}{\partial x}\right|_{x=r} = -R_{ab} \tag{8c}$$

$$\left.\frac{\partial h}{\partial x}\right|_{x=s} = \begin{cases} D(x,t)\dfrac{ds}{dt}, & \dfrac{ds}{dt} > 0 \\ 0, & \dfrac{ds}{dt} \leq 0 \end{cases}. \tag{8d}$$

The initial conditions are:

$$s(t=0) = r(t=0) = 0. \tag{9}$$

In the particular case in which the shoreline only migrates seawards (i.e., $ds/dt > 0$), the system maintains the wedge geometry depicted in Figures 1a and 2a, and we can define the basin depth as $D(x,t) = s + Z$ (Lorenzo-Trueba et al., 2013). Under this special case, equations (7) – (9) admit closed form analytical solutions, which are described in section 4. In general, however, these equations require a numerical solution.

Model Variables

Symbol	Units	Description	Dimensionless Symbol
t	T	time	t
x	L	horizontal distance	x
h	L	height above current sea-level	h
r	L	alluvial-bedrock transition horizontal distance from origin	r
s	L	shoreline horizontal distance from origin	s
q	L^2T^{-1}	sediment flux	q
Z	L	sea-level	Z
H	-	enthalpy	H
L	-	latent heat	L

Parameters

Symbol	Units	Description	Dimensionless Symbol
q_0	L^2T^{-1}	Sediment flux at ABT	
ν	L^2T^{-1}	fluvial diffusivity	R_{ab}
β	-	basement slope	
ψ	-	foreset slope	Rsh
$\dot{z}$	L^2T^{-1}	Rate of sea-level change	$\dot{z}$

3 The Geomorphic Enthalpy Method

We develop a numerical solution of the problem able to operate in cases where the closed form solutions do not hold. The solution used here is an adaptation of the fixed grid enthalpy-like solution proposed by Lorenzo-Trueba and Voller (2010), which requires an enthalpy function defined as:

$$H = h + L(x,t). \tag{10}$$

In this case, however, the latent heat term L is a function of both space (a variable ocean basement depth) and time (a variable sea level). Taking account of the dimensionless variable definitions in (4), we define L as:

$$L = \begin{cases} x + Z, & x > 0 \\ Z, & x \leq 0 \end{cases}. \tag{11}$$

As long as the shoreline only migrates seawards, the formulation in equations (10) and (11) is applicable throughout the entire domain (fluvial and submarine). When the shoreline retreats, however, the enthalpy function stores the sediment thickness information in the submarine domain without satisfying equation (10) (i.e., $h = 0$ and $H < L$; see Figure 3b). In this way, the numerical solution can account for shoreline progradation after shoreline retreat (see Results sections).

Using this enthalpy function described in equation (10), the problem can be described as a single Exner sediment balance equation for the full solution space as

$$\frac{\partial H}{\partial t} = \frac{\partial q}{\partial x}, \qquad -\infty. < x < \infty. \tag{12}$$

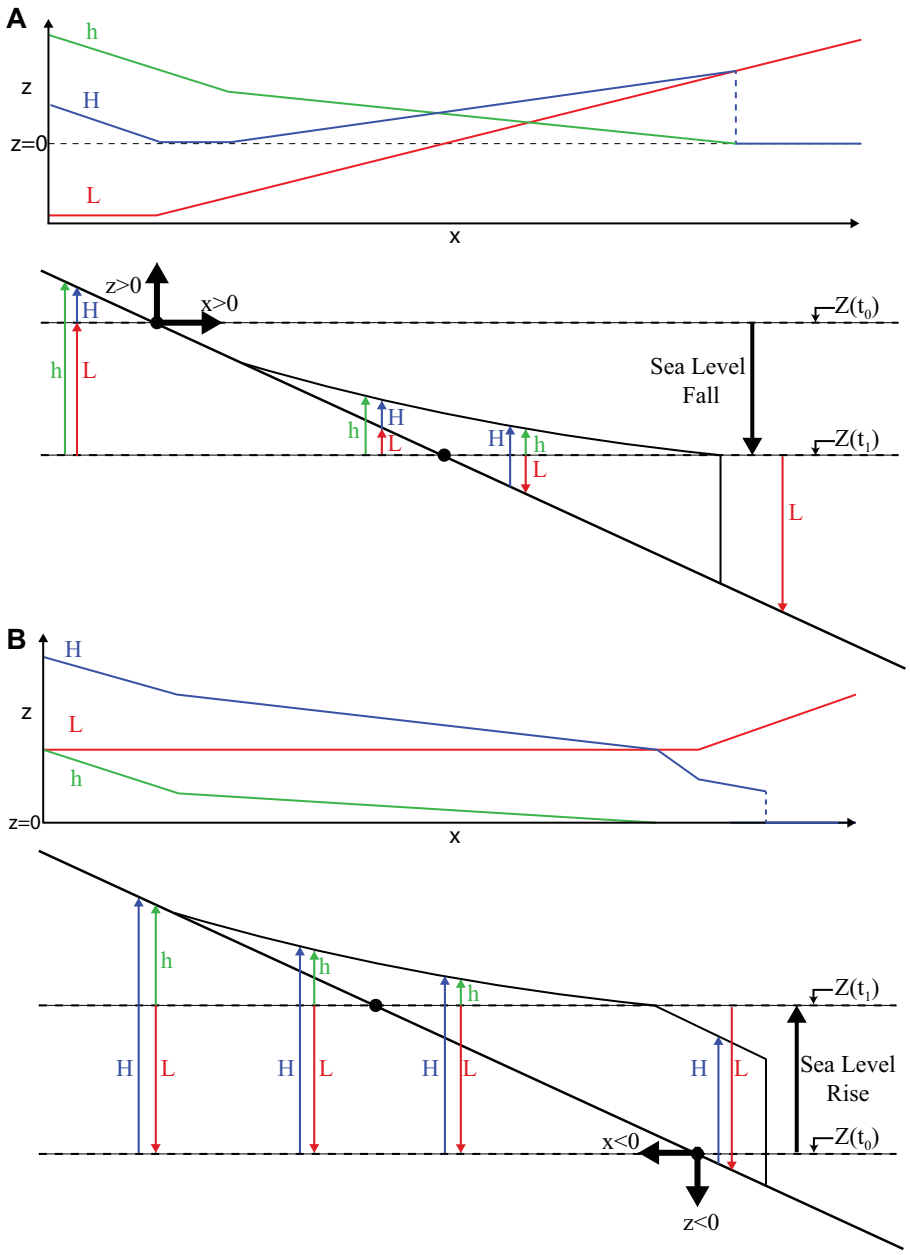

Figure 3: Model variables under a general (a) sea-level fall and (b) sea-level rise scenario.

The formulation of the sediment flux, q, however, cannot be applied throughout the entire domain. We impose a non-erodible condition for the basement, which requires separating the domain into two regions: upstream and downstream of the ABT (Figure 4b). Upstream of the ABT the sediment is bypassed (i.e., there is neither erosion or deposition), whereas downstream of the ABT sediment transport is proportional to the local slope $S = -\partial h/\partial x$. In this way, taking account of the dimensionless variable definitions in (4), we define q as:

$$q = \begin{cases} R_{ab}, & x < r \\ S, & x \geq r \end{cases} . \tag{13}$$

We note that the formulation introduced by equation (13) departs from the formulation introduced by Lorenzo-Trueba and Voller (2010) (i.e., $q = \min(R_{ab}, S)$), which is applied to the entire domain. This formulation only works when the fluvial profile is always concave upward and the sediment flux q is bounded above by R_{ab}. In the more general case presented, however, sea-level variations can result in changes in concavity and inflexion points in the fluvial surface.

The boundary conditions for (12) are:

$$\lim_{x\to-\infty} q = R_{ab} \tag{14a}$$

$$\lim_{x\to\infty} h = 0 \tag{14b}$$

and the initial conditions are

$$H = h = \begin{cases} 0, & x > 0 \\ -x, & x \leq 0 \end{cases} \tag{15}$$

and, inverting (10),

$$h = \max(H - L, 0). \tag{16}$$

We develop a numerical solution of Eq. (10) to (16) based on a uniform grid size Δx, and the origin point $x = 0$ located at the interface between two nodes, the most landward node indexed to be $i = 1$, and as we move seaward the node index increases. In this way, the location of any node is given by

$$x_i = (i - 0.5) \cdot \Delta x. \tag{17}$$

Additionally, we use uniform time step size Δt and use index j to indicate the time step. The explicit time integration finite difference form of (12) is

$$H_{i,j+1} = H_{i,j} + \frac{\Delta t}{\Delta x} \cdot \left(q_{i+\frac{1}{2},j} - q_{i-\frac{1}{2},j} \right) \tag{18}$$

where the subscript $j + 1$ refers to values at the new time step, subscript $i + 1/2$ refers to the interface between nodes i and $i+1$. In this way, and based on equation (13), the flux from node i to node $i + 1$ is approximated as

$$q_{i+\frac{1}{2},j} = \begin{cases} R_{ab}, & i \leq K_j + 1 \\ S_{i,j}, & i > K_j + 1 \end{cases} \tag{19}$$

where $S_{i,j} = (h_{i-1,j} - h_{i,j})/\Delta x$ and K_j is the cell where the ABT is located at time step j. Both $S_{i,j}$ and K_j are updated at each time step based on the sediment flux at the ABT, $q_{ABT} = q_{K_j,j}$. q_{ABT} is bounded above by the basement slope, which taking account of the dimensionless variable definitions in (4) is equal to 1 (Figure 4). Consequently, when the condition $q_{ABT} > 1$ is satisfied, the ABT migrates one cell seawards to prevent the basement from being eroded. Additionally, q_{ABT} is bounded below by the upstream sediment input, which taking account of the dimensionless variable definitions in (4) is equal to R_{ab} (Figures 4c and 4d). Thus, when the condition $q_{ABT} < R_{ab}$ is satisfied, the ABT migrates one cell landwards. The ABT remains in the same cell when $R_{ab} \leq q_{ABT} \leq 1$.

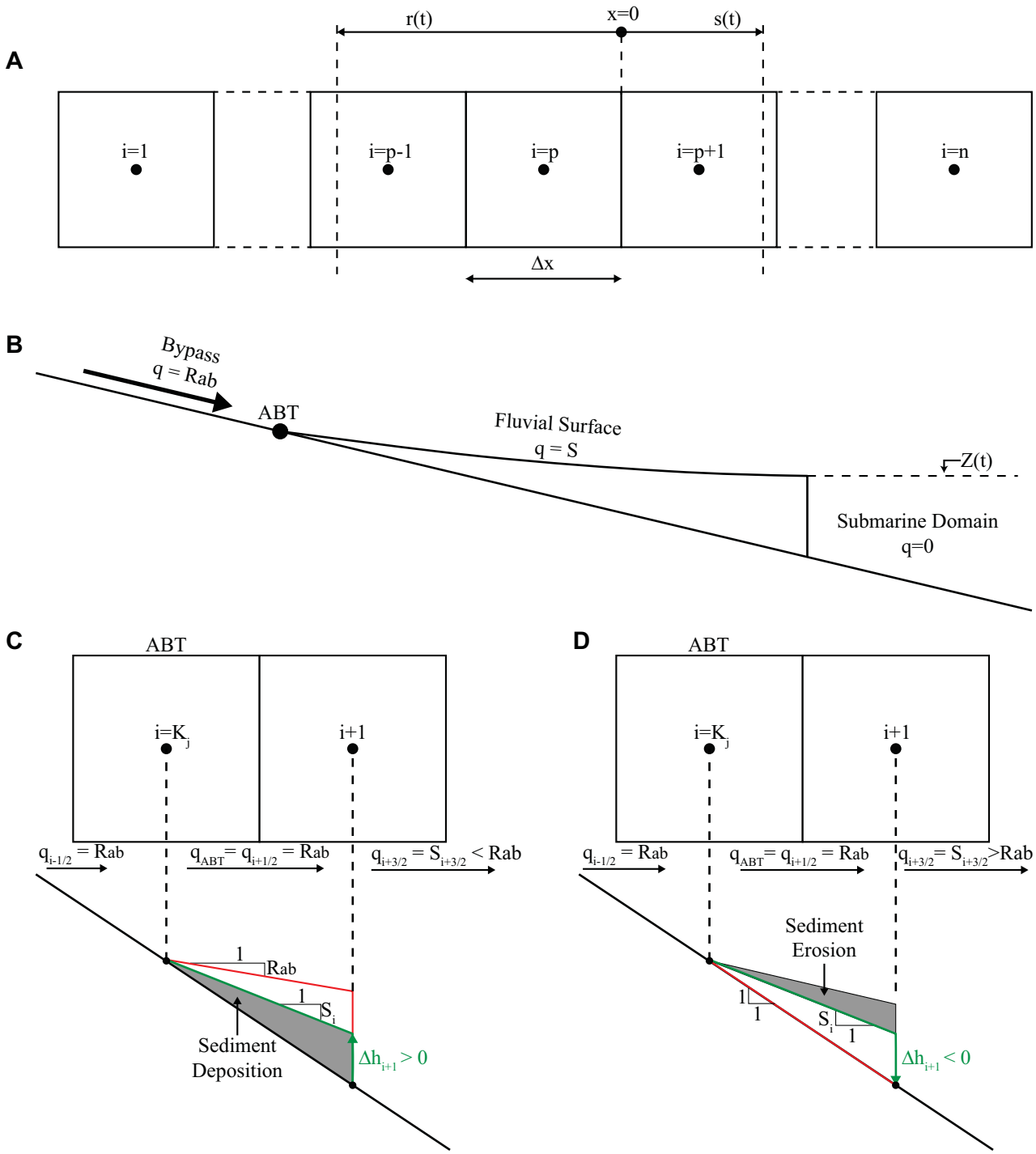

Figure 4: Depiction of (a) discrete domain, (b) sediment transport regimes in the model domain, (c) numerical criteria for ABT landward migration, (d) numerical criteria for ABT seaward migration.

In order to guarantee stability, the time and space steps need to satisfy $\Delta t/\Delta x^2 < 0.5$. To meet this stability criterion, we use a space step Δx and a time step in the range $10^{-5} \leq \Delta t \leq 5 \cdot 10^{-5}$. At each time step, the solution of (18) explicitly provides new values for the sediment thickness $H_{i,j+1}$ at each node. New time step

values for the sediment heights $h_{i,j+1}$ are then calculated from the discrete form of (16). Additionally, the ABT position is then determined by interpolation between nodes $i+1$ and i as follows:

$$r_j = \frac{h_{i+1,j} + Z_j - R_{ab} \cdot x_{i+1}}{1 - R_{ab}}. \tag{20}$$

This provides sufficient information to recalculate the fluxes in (19) and propagate the solution of (18) forward in time.

We also estimate the location of the SH at each time step. Under SH progradation, the current total sediment field $H_{i,j}$ is searched, and the first node i where $0 < H_{i,j} < L_{i,j}$ is located. The SH position is then determined by interpolation through the control volume around node i, i.e.,

$$s_j = (i-1)\Delta x + \frac{H_{i,j}}{L_{i,j}}\Delta x. \tag{21}$$

4 Verification of the Enthalpy Method

We verify the proposed model under two sea-level change scenarios that admit closed form analytical solutions: square root sea-level rise and fall, and constant sea-level rise.

4.1 Square root sea-level rise and fall

Under sea-level rise proportional to the square root of time i.e. $Z = 2\lambda_Z\sqrt{t}$, Lorenzo-Trueba et al. (2013) developed an analytical similarity solution in which the movements of the ABT and SH are given by equations of the form:

$$r = -2\lambda_{ab}\sqrt{t} \tag{22a}$$

$$s = 2\lambda_{sh}\sqrt{t} \tag{22b}$$

where λ_{ab} and λ_{sh} are constants determined through two algebraic equations (Lorenzo-Trueba et al., 2013).

We use this analytical solution to assess accuracy of the enthalpy method under a wide range of R_{ab} and λ_Z values. Figure 5 shows plots of the SH and ABT trajectories over time for two values of R_{ab} during sea-level fall. In both scenarios there is agreement between the analytical and numerical solutions. Depending on values of these two parameters the delta can undergo coastal offlap or coastal onlap during sea-level fall. The profile evolutions in figure 5 illustrate concavity differences in the fluvial surface that are a result of the direction of ABT migration. In scenarios of sea-level fall proportional to the square root of time, larger values of R_{ab} or smaller values of λ_Z result in coastal onlap and a concave up fluvial surface. However, significantly decreasing R_{ab} or increasing the magnitude of λ_Z causes the delta to undergo coastal offlap and produces a concave down fluvial surface. During costal offlap sediments are reworked in the upstream portion of the delta and provided to the rest of the system causing sediment flux values in the fluvial surface to exceed R_{ab} and resulting in the concave downward profile. Model runs for several values of R_{ab} and λ_Z are included in figures A1 and A2.

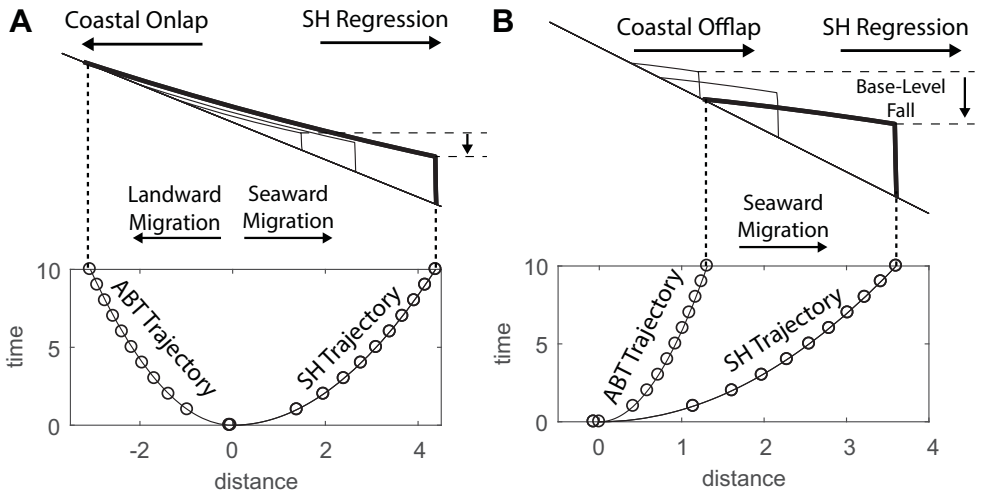

Figure 5: Examples of delta evolution during sea-level fall with (a) high R_{ab} and (b) low R_{ab}. On the bottom is a comparison of boundary trajectories of the analytical (solid-lines) and numerical (circles) solutions. The top shows the development of the longitudinal profile over time.

A further test of the robustness of the enthalpy solution is revealed by investigating its performance across the entire feasible range of the ABT slope ratio $0 < R_{ab} < 1$; in each case the value of λ_Z is set proportional to λ_{sh}. First, the analytical solution in Lorenzo-Trueba et al. (2013) is used to predict values of λ_{ab} and λ_{sh}. Then, we extract the values of λ_{ab} and λ_{sh} at specific values of $R_{ab}[0.05 : 0.05 : 0.85]$ through fitting the forms in (10) to the predicted trajectories r and s given by the enthalpy solution. Benchmarks are made for both a sea-level rise (e.g., $\lambda_Z = 0.5\lambda_{sh}$) and a sea-level fall (e.g., $\lambda_Z = -0.5\lambda_{sh}$). In Figure 6 we present a comparison of the analytical values of the moving boundary parameters (solid-line) with those predicted by the enthalpy method (shapes). We find that

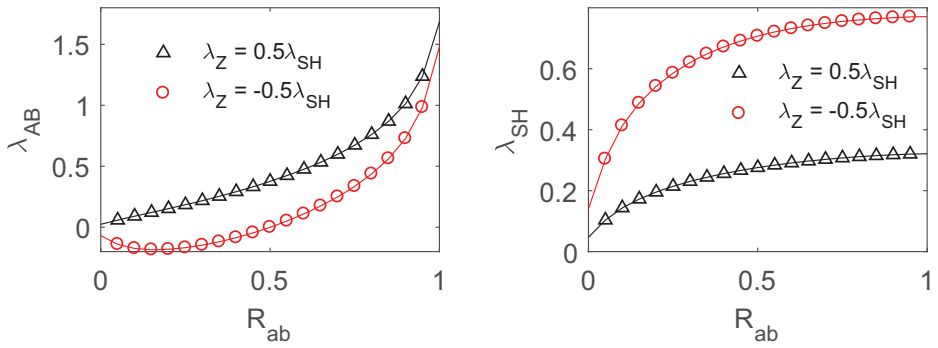

Figure 6: Comparison between analytical and time stepping predictions of the moving boundary parameters λ_{sh} and λ_{ab} for the sea-level fall (in red) and sea-level rise (black) scenarios. The solid-line is the analytical solution and the symbols represent the enthalpy numerical solution described in section 4. For $R_{ab} < 0.9$ we use $\Delta x = 0.01$ and $\Delta t = 5 \cdot 10^{-5}$. For $R_{ab} \geq 0.9$ we use $\Delta x = 10^{-3}$ and $\Delta t = 5 \cdot 10^{-7}$.

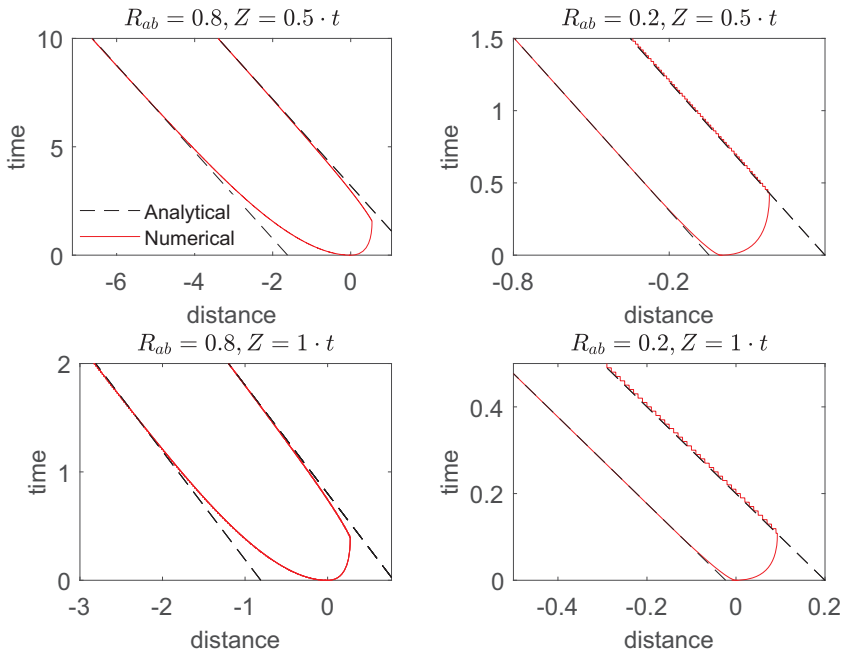

Figure 7: Comparison of analytical (dashed) and numerical (solid) ABT and SH trajectories under constant sea-level rise with $\Delta x = 0.01$ and $\Delta t = 5 \cdot 10^{-5}$.

across a wide range of conditions the time stepping solution matches the analytical solution.

4.2 Constant Sea-Level Rise

Under constant sea-level rise rate $\dot{Z}$ (i.e. sea-level is described by $Z = \dot{z} \cdot t$), the system can reach a point in which the incoming sediment flux is insufficient to supply the foreset (Muto, 2001; Parker and Muto, 2003), which results in the fluvial plain abandoning the submarine portion (Figure 2b). When this happens, the system first enters a transition period in which the length of the fluvial plain increases and both the ABT and the SH migrate landwards. This transition period ends when the fluvial surface attains a fixed geometry, and both the ABT and the SH attain a constant landward migration rate. Once the fluvial surface achieves this fixed length, we define the boundaries of the fluvial surface, by:

$$s^* = s_i - \dot{z}t \tag{23a}$$

$$r^* = r_i - \dot{z}t \tag{23b}$$

where s_i and r_i are constants determined by:

$$s_i = \frac{R_{ab}}{\dot{z}} \tag{24a}$$

$$r_i = \frac{1}{\dot{z}}[R_{ab} + \ln(1 - R_{ab})]. \tag{24b}$$

A full derivation of this solution is included in the Appendix.

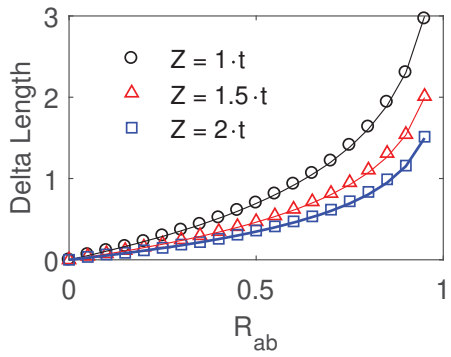

Figure 8: Comparison of analytical (solid lines) and numerical (symbols) delta lengths once a fixed length is reached for the fluvial surface. For several magnitudes of constant sea-level rise there is agreement between both solutions.

We use this analytical solution to test the fixed grid numerical scheme for a wide range of R_{ab} and $\dot{Z}$ values. Figure 7 shows plots of the movement of the SH and ABT over time. We find that the trajectories predicted by the enthalpy solution (solid-lines) eventually match the analytical solution (dashed-line).

Additionally, a further test of the robustness of the enthalpy solution is revealed by investigating its performance across the entire feasible range of the ABT slope ratio $0 < R_{ab} < 1$. In particular, we calculate the length of the fluvial surface at steady state (i.e., $s - r$) for specific values of $R_{ab}[0.05 : 0.05 : 0.95]$, using the enthalpy solution and the analytical solution (equation (A7)). In Figure 8 we present a comparison of the analytical values of the moving boundary parameters (solid-line) with those predicted by the enthalpy method (shapes). We find that across a wide range of conditions the time stepping solution matches the analytical solution.

5 Predictions under sea-level change scenarios

To demonstrate how the proposed enthalpy method can be used to understand delta dynamics under sea-level change conditions, we consider more general cases than those investigated in the model verification. In particular, we investigate the dynamics of the delta boundaries (SH and ABT) under sinusoidal sea-level cycles, i.e.,

$$Z = A\sin(B \cdot t). \tag{25}$$

An interesting feature under sea-level cycles is that the SH can reverse its direction of migration. During these reversals, the geometric configuration of the system shifts between the one shown in Figure 2a, in which wedge geometry is maintained, and Figure 2b, in which the foreset and the fluvial plain abandons the submarine portion (i.e., autobreak). This is well illustrated in Figures 9 and 10, which demonstrate that the enthalpy method can therefore account for transgression (e.g., a landwards migration of the SH) followed by regression (e.g., a seawards migration of the SH) and vice versa. In particular, Figure 9 includes the ABT and SH trajectories, and Figure 10 includes the stratigraphy produced

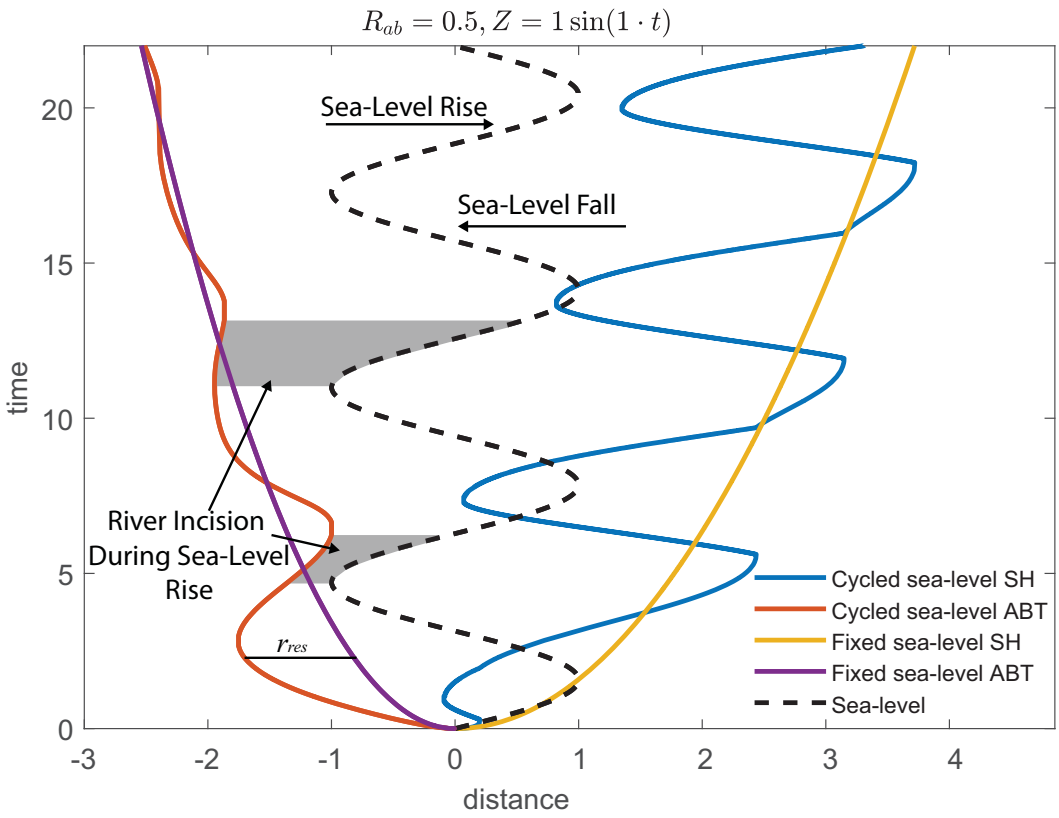

Figure 9: ABT and SH trajectories under sea-level cycles (i.e., $Z = \sin(t)$ and $R_{ab} = 0.5$.

under a range of R_{ab} values.

The model predicts interesting stratigraphic features under sea-level cycles. It is possible for the shape of an older sediment layer to be affected by new sediment deposits, producing lenses in the stratigraphy. During sea-level fall the upstream end of an older sediment layer has the potential to be eroded away, and downstream an older layer can be truncated by newly forming sediment layers. These lenses are a result of curvature changes in the fluvial surface, something that cannot be captured by models which assume a linear fluvial surface (Kim and Muto, 2007). The stratigraphies in figure 10 also demonstrate how changing R_{ab} affects the amount of sediment that is preserved in the delta under sea-level cycles. In particular, increasing the value of R_{ab} causes an increase in the amount of sediment preserved by the system.

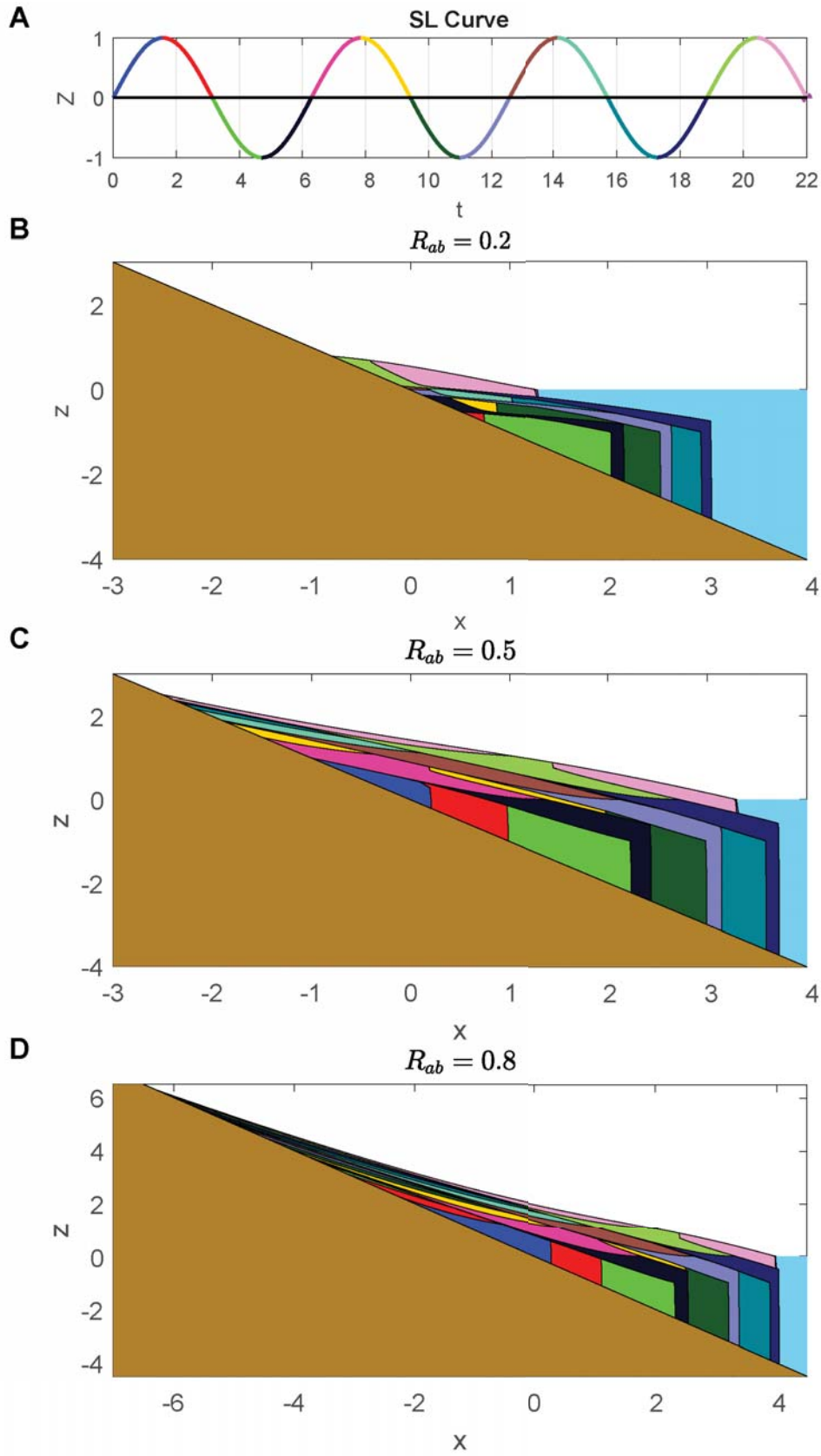

Figure 10: Stratigraphies produced under base-level cycling for three different values of $R_{ab} = q/\beta\nu$.

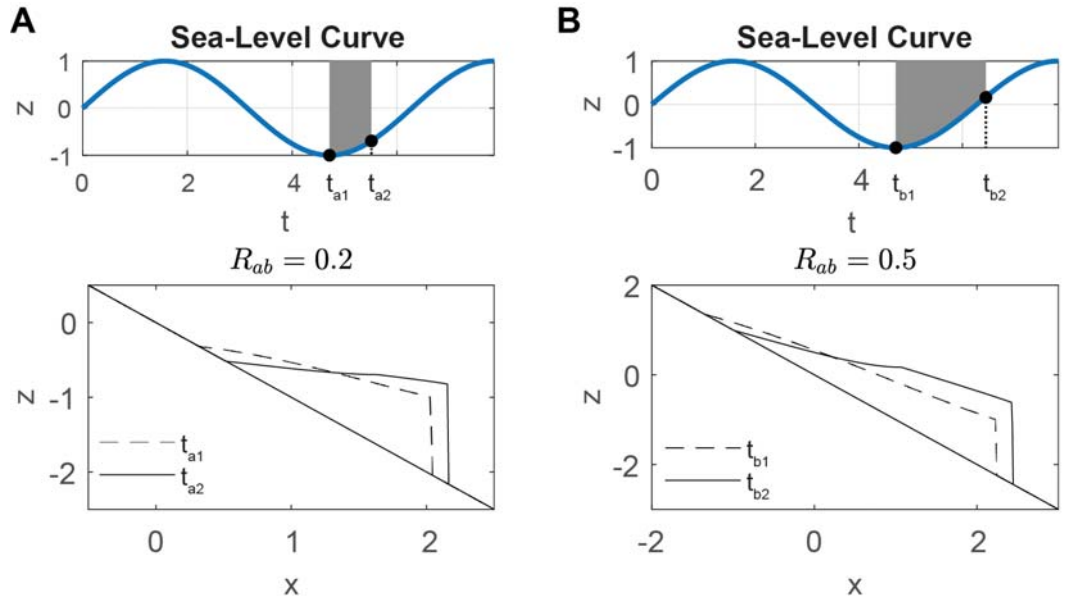

Figure 11: Profiles plotted at the start and end of river incision during sea-level rise. River incision for a higher R_{ab} value in (b) lasted for a longer time than with the lower R_{ab} value in (a). Under higher R_{ab} values such as 0.8, this sea-level cycle does not have a high enough amplitude to cause any periods of coastal offlap.

6 Time Lags in Fluvial Response to Sea-Level Change

Another interesting feature to explore in this section is the ABT response to the driving sea-level signal. To do this, we define a residual ABT, r_{res}, as the difference between the ABT response to base-level cycles and the corresponding trajectory under a fixed sea-level. The residual trajectories are then plotted with the sea-level curve, seen in Figure 12a. As in Swenson et al. (2000) we find that ABT response is attenuated continuously with basin age.

For this section we convert back from dimensionless units by assuming a fixed length scale $l = 100$km, diffusivity $\nu = 10^6 \mathrm{m}^2\mathrm{y}^{-1}$, and basement slope $\beta = 10^{-3}$, which are representative values of sedimentary basins in humid climates (Swenson et al., 2000). With these values fixed an increase in R_{ab} corresponds to an increase in sediment supply. In order to test the effect of sediment supply on the time lags in ABT response to sea-level changes, we run the model for three different amplitudes of sea-level cycles under a wide range of R_{ab} values $R_{ab}[0.2 : 0.05 : 0.8]$. Although a delay in ABT response exists whenever there is a shift between sea-level rise and fall, we look specifically at the first transition from sea-level fall to rise in the cycle (Figure 12a).

Figure 12b shows the time delay across a range of sediment supply values. The model suggests that increasing sediment supply to the delta increases the delay in ABT reponse to changes in the directions of sea-level migration; a behavior which has important consequences in the reconstruction of past sea-levels. Under certain conditions it may take thousands of years for any changes in the direction of sea-

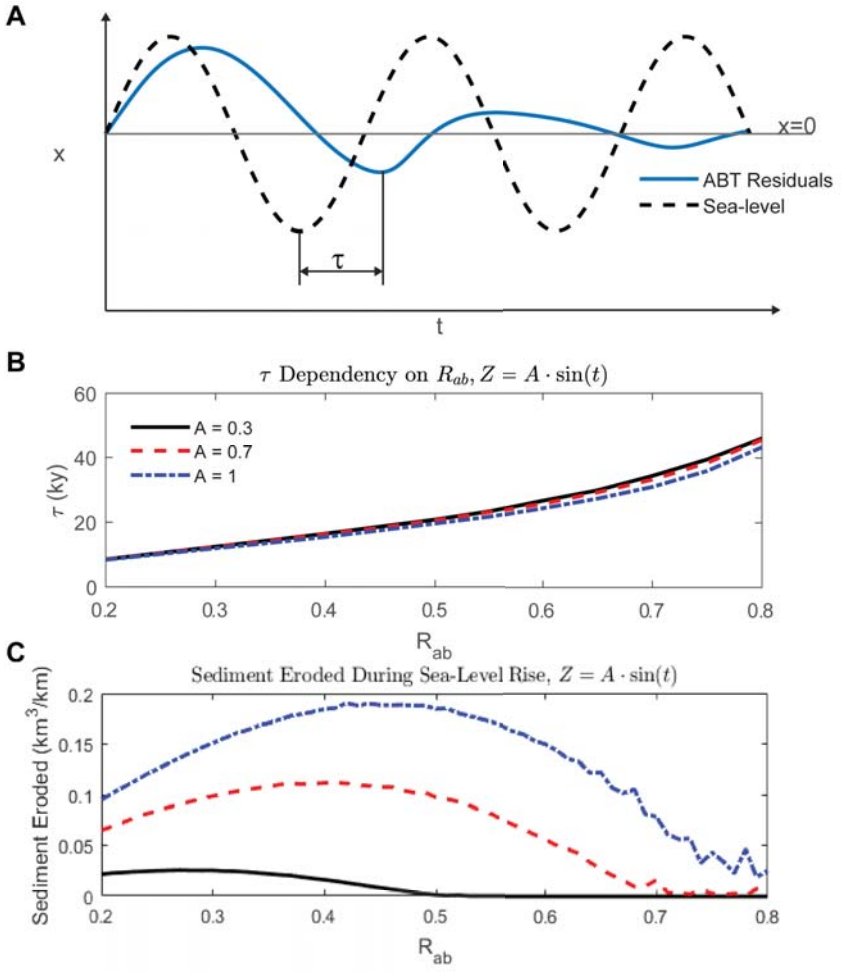

Figure 12: (a) Residual ABT response to sea-level cycling. Refer to Figure 9, which depicts the residuals. (b) Time delay between the sea-level changing direction and the residual ABT curve changing direction. (c) Volume eroded at the ABT during sea-level rise.

level migration to cause a change in direction of ABT migration, meaning that seaward migration of the ABT cannot be used as a direct indicator of sea-level fall.

We also measure volume eroded in the upstream portion of the delta during sea-level rise. Figure 12c shows the amount of volume eroded increases as the amplitude of the sea-level cycle increases. An interesting behavior is that the maximum amount of erosion occurs near the middle of feasible R_{ab} values, which is a result of allowing curvature in the fluvial surface. For low R_{ab} values the fluvial surface is not long enough to allow large changes in curvature, resulting in the system responding to sea-level changes relatively quickly. Conversely, large R_{ab} values provide enough sediment that the delta is able to better withstand any effects of changing sea-level. Thus, the largest amount of curvature change occurs closer to the center of possible R_{ab} values when the fluvial surface is long enough but not able to withstand sea-level changes well.

7 Conclusions

We have developed an extension of the enthalpy method that is able to account for changes in base-level. This numerical solution shows agreement with existing analytical solutions for sea-level change proportional to the square root of time and constant sea-level rise. Accounting for sea-level change allows this to be the first version of the enthalpy method that is able to capture behaviors such as landward migration of the ABT and cycles of SH regression and transgression.

The model results have important geological consequences. Under sea-level cycles the curvature of the fluvial surface is able to produce lenses in the stratigraphy due to erosion of older sediment layers. Additionally, there is a delay between changes in the direction of sea-level migration and changes in the direction of ABT migration. This delay must be accounted for in attempt to reconstruct past sea-levels from the ABT.

Future work will extend the geomorphic enthalpy model into two dimensions. Other models have considered solving the one-dimensional delta problem with the use of a deforming grid, where the boundaries are fixed through a transformation. This complicates the governing equations and would be difficult to implement in 2D. The enthalpy method does not create these complications and should have a natural extension to the two-dimensional problem.

It may be interesting to look at the effect of sediment supply cycles on the boundary trajectories. All runs included in this paper were carried out with a constant R_{ab} values, but the model allows for R_{ab} to be dependent on time.

References

Capart, H., Bellal, M., Young, D.-L., 2007. Self-Similar Evolution of Semi-Infinite Alluvial Channels with Moving Boundaries. J. Sediment. Res. 77, 13–22. https://doi.org/10.2110/jsr.2007.009

Crank, J., 1984. Free and Moving Boundary Problems. Oxford Press.

Edmonds, D.A., Paola, C., Hoyal, D.C.J.D., Sheets, B.A., 2011. Quantitative metrics that describe river deltas and their channel networks. J. Geophys. Res. Earth Surf. 116, 1–15. https://doi.org/10.1029/2010JF001955

Fagherazzi, S., Overeem, I., 2007. Models of Deltaic and Inner Continental Shelf Landform Evolution. Annu. Rev. Earth Planet. Sci. 35, 685–715. https://doi.org/10.1146/annurev.earth.35.031306.140128

Kim, W., Muto, T., 2007. Autogenic response of alluvial-bedrock transition to base-level variation: Experiment and theory. J. Geophys. Res. Earth Surf. 112, 1–13. https://doi.org/10.1029/2006JF000561

Lai, S.Y.J., Capart, H., 2007. Two-diffusion description of hyperpycnal deltas. J. Geophys. Res. Earth Surf. 112. https://doi.org/10.1029/2006JF000617

Lorenzo-Trueba, J., Voller, V.R., 2010. Analytical and numerical solution of a generalized Stefan problem exhibiting two moving boundaries with application to ocean delta formation. J. Math. Anal. Appl. 366, 538–549. https://doi.org/10.1016/j.jmaa.2010.01.008

Lorenzo-Trueba, J., Voller, V.R., Muto, T., Kim, W., Paola, C., Swenson, J.B., 2009. A similarity solution for a dual moving boundary problem associated with a coastal-plain depositional system. J. Fluid Mech. 628, 427–443. https://doi.org/10.1017/S0022112009006715

Lorenzo-Trueba, J., Voller, V.R., Paola, C., 2013. A geometric model for the dynamics of a fluvially dominated deltaic system under base-level change. Comput. Geosci. 53, 39–47. https://doi.org/10.1016/j.cageo.2012.02.010

Marr, J.G., Swenson, J.B., Paola, C., Voller, V.R., 2000. A two-diffusion model of fluvial stratigraphy in closed depositional basins. Basin Res. 12, 381–398. https://doi.org/10.1111/j.1365-2117.2000.00134.x

Muto, T., 2001. Shoreline autoretreat substantiated in flume experiments. J. Sediment. Res. 71, 246–254. https://doi.org/10.1306/091400710246

Muto, T., Steel, R.J., 2002. Role of autoretreat and A/S changes in the understanding of deltaic shoreline trajectory: A semi-quantitative approach. Basin Res. 14, 303–318. https://doi.org/10.1046/j.1365-2117.2002.00179.x

Paola, C., 2000. Quantitative models of sedimentary basin filling. Sedimentology. https://doi.org/10.1046/j.1365-3091.2000.00006.x

Paola, C., Heller, P.L., Angevine, C.L., 1992. The large-scale dynamics of grain-size variation in alluvial basins, 1: Theory. Basin Res. 4, 73–90. https://doi.org/10.1111/j.1365-2117.1992.tb00145.x

Paola, C., Voller, V.R., 2005. A generalized Exner equation for sediment mass balance. J. Geophys. Res. Earth Surf. 110, 1–8. https://doi.org/10.1029/2004JF000274

Parker, G., Muto, T., 2003. 1D numerical model of delta reponse to rising sea level. 3rd IAHR Symp. River, Coast. Estuar. Morphodynamics 1–10.

Parker, G., Muto, T., Akamatsu, Y., Dietrich, W.E., Lauer, J.W., 2008. Unravelling the conundrum of river response to rising sea-level from laboratory to field. Part I: Laboratory experiments. Sedimentology 55, 1643–1655. https://doi.org/10.1111/j.1365-3091.2008.00961.x

Posamentier, H.W., Allen, H.W., James, D.P., Tesson, M., 1992. Forced regression in a sequence stratigraphic framework: Concepts, examples, and sequence stratigraphic significance. Am. Assoc. Pet. Geol. Bull. 76, 1687–1709.

Postma, G., Kleinhans, M.G., Meijer, P.T.H., Eggenhuisen, J.T., 2008. Sediment transport in analogue flume models compared with real-world sedimentary systems: A new look at scaling evolution of sedimentary systems in a flume. Sedimentology 55, 1541–1557. https://doi.org/10.1111/j.1365-3091.2008.00956.x

Swenson, J.B., Muto, T., 2007. Response of coastal plain rivers to falling relative sea-level: Allogenic controls on the aggradational phase. Sedimentology 54, 207–221. https://doi.org/10.1111/j.1365-3091.2006.00830.x

Swenson, J.B., Voller, V.R., Paola, C., Parker, G., Marr, J.G., 2000. Fluviodeltaic sedimentation: A generalized Stefan problem. Eur. J. Appl. Math. 11, 433–452. https://doi.org/10.1017/S0956792500004198

Voller, V.R., Swenson, J.B., Kim, W., Paola, C., 2006. An enthalpy method for moving boundary problems on the earth's surface. Int. J. Numer. Methods Heat Fluid Flow 16, 641–654. https://doi.org/10.1108/09615530610669157

Voller, V.R., Swenson, J.B., Paola, C., 2004. An analytical solution for a Stefan problem with variable latent heat. Int. J. Heat Mass Transf. 47, 5387–5390. https://doi.org/10.1016/j.ijheatmasstransfer.2004.07.007

A An appendix

A.1 Closed-Form Solution Under Constant Sea-level Rise

We assume a constant sea-level rise rate Z, (i.e., sea level is described as $Z = \dot{z}t$). On setting the similarity variable

$$\xi = x + \dot{z}t \tag{A1}$$

scaling the sediment height by

$$\eta = h - \dot{z}t \tag{A2}$$

and defining the following boundaries

$$s^* = s_i - \dot{z}t \tag{A3a}$$
$$r^* = r_i - \dot{z}t. \tag{A3b}$$

Therefore, the similarity solution becomes

$$\frac{d^2\eta}{d\xi^2} - \dot{z}\frac{d\eta}{d\xi} - \dot{z} = 0, \qquad r^* \leq \xi \leq s^* \tag{A4}$$

with boundary conditions

$$\eta\Big|_{\xi=s^*} = 0 \tag{A5a}$$
$$\eta\Big|_{\xi=r^*} = -r^* \tag{A5b}$$
$$\frac{\partial\eta}{\partial\xi}\Big|_{\xi=r^*} = -R_{ab} \tag{A5c}$$
$$\frac{\partial\eta}{\partial\xi}\Big|_{\xi=s^*} = 0. \tag{A5d}$$

On satisfying (A4), (A5a), and (A5d) we obtain the following solution

$$\eta = \frac{1}{\dot{z}}\exp(\dot{z}\xi - \dot{z}s^*) - \xi + \frac{R_{ab} - 1}{\dot{z}} \tag{A6a}$$
$$h = \frac{1}{\dot{z}}\exp(\dot{z}x - \dot{z}s) - x + \frac{R_{ab} - 1}{\dot{z}} \tag{A6b}$$

From (A2) and (A5) we obtain the values of s^*, and r^*

$$s^* = \frac{R_{ab}}{\dot{z}} \tag{A7a}$$
$$r^* = \frac{1}{\dot{z}}[R_{ab} + \ln(1 - R_{ab})] \tag{A7b}$$

Thus, the length of the fluvial surface can be calculated as

$$s^* - r^* = s_i - r_i = \frac{\ln(1 - R_{ab})}{\dot{z}} \tag{A8}$$

A.2 Additional verification of the enthalpy method.

In this section, we include further tests of the fixed grid numerical scheme. In particular, Figures A1 and A2 show trajectories of the SH and ABT over time for a wide range of R_{ab} and λ_Z values. We note that under sea-level fall it is possible for the ABT to migrate landward or seaward depending on the R_{ab} value (Figure A2). We find that the numerical solution matches the analytical solution in all cases.

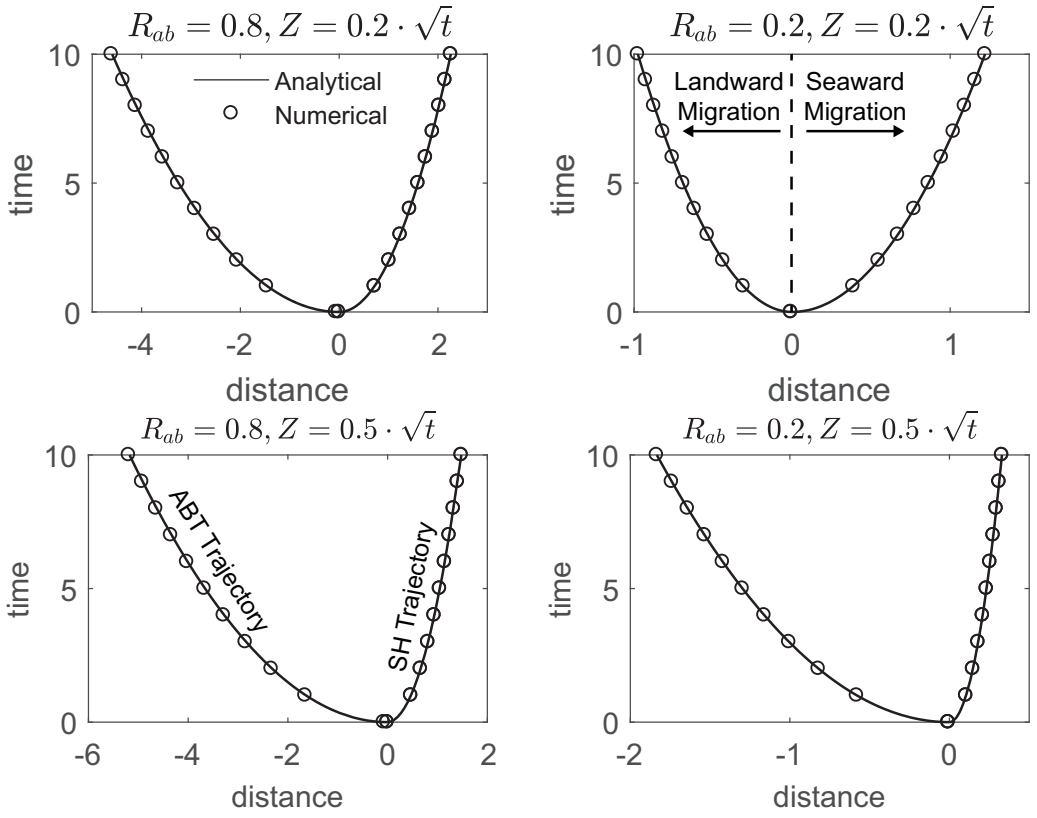

Figure A1: Comparison of analytical (solid lines) and numerical (circles) ABT and SH trajectories under square root sea-level rise.

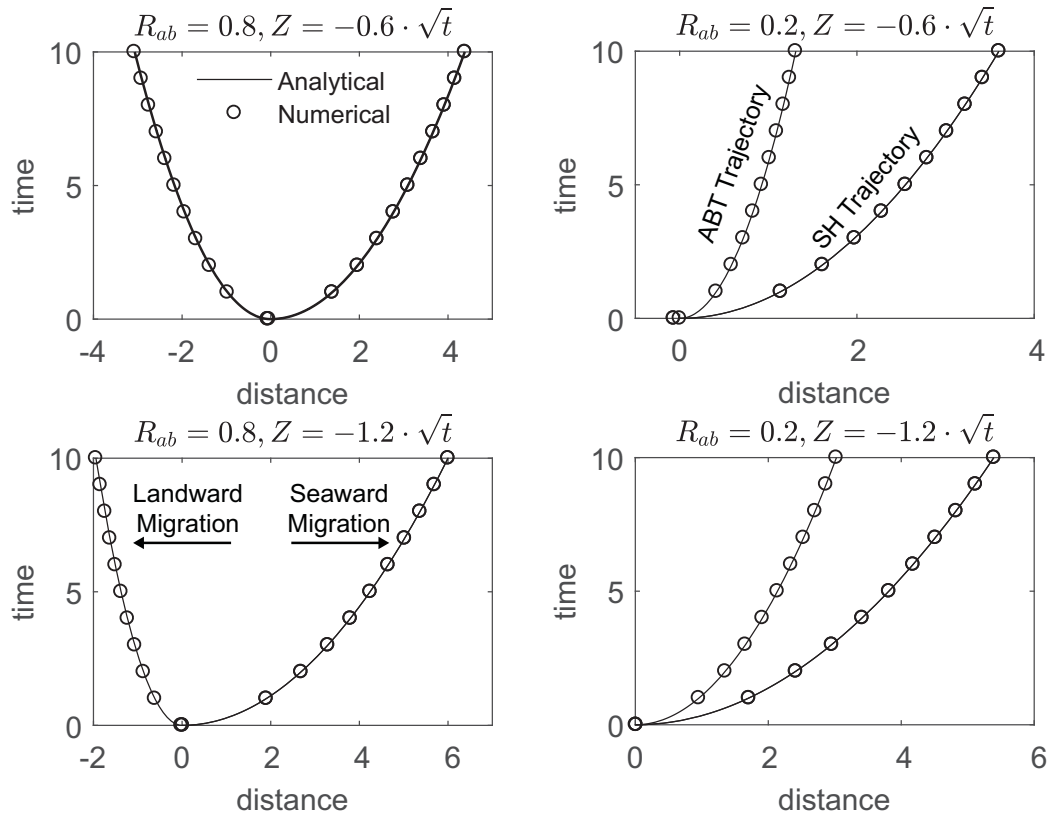

Figure A2: Comparison of analytical (solid lines) and numerical (circles) ABT and SH trajectories under square root sea-level fall.